Research article

Silver coated PS microsphere array SERS microfluidic chip for pesticide detection

Wang Peng [a,b,c,d,e,*], Zhihan Xu [a], Chao Yi [a], Yuankai Zhang [a], Qingxi Liao [a,d,**]

[a] College of Engineering, Huazhong Agricultural University, Wuhan, 430070, China
[b] Shenzhen Branch, Guangdong Laboratory for Lingnan Modern Agriculture, Genome Analysis Laboratory of the Ministry of Agriculture, Agricultural Genomics Institute at Shenzhen, Chinese Academy of Agricultural Sciences, Shenzhen, 518000, China
[c] Shenzhen Institute of Nutrition and Health, Huazhong Agricultural University, Wuhan, 430070, China
[d] Key Laboratory of Agricultural Equipment in Mid-Lower Yangtze River, Ministry of Agriculture and Rural Affairs, Wuhan, 430070, China
[e] The Center of Crop Nanobiotechnology, Huazhong Agricultural University, Wuhan, 430070, China

ARTICLE INFO

ABSTRACT

Carbendazim and acetamidine are pesticides that widely used to control pests and diseases in oilseed rape. In this paper, a rapid, accurate and reliable method was proposed for the detection of carbendazim and acetamidine with SERS microfluidic chip technology. Ag-ps(Polystyrene microspheres) microsphere SERS substrate was prepared by spin coating and magnetron sputtering deposition of Ag. The enhancement factor of prepared SERS substrate was 2.4×10^{10}. The SERS detection working curves were well fitted and the linear parameters R^2 were 0.987 and 0.994, respectively. The limit of detection was 0.01 mg/mL. The use of SERS microfluidic chip to detect carbendazim and acetamidine is expected to provide a way for the detection of pesticide residues in crops, which has broad application prospects in the field of food safety.

1. Introduction

The use of pesticides can prevent oilseed rape from being harmed by diseases, pests and grasses, so as to ensure crop yield and quality [1–4]. Pesticide used in rape plant may lead to pesticide residues in rapeseed, among which organophosphorus pesticides are widely used. Organophosphorus pesticides have the characteristics of wide range, high efficacy and short half-life, which have been widely used in rape planting. In order to control the production of pests and weeds, pesticides are used heavily, about 4 kg per hectare. This will bring a series of problems, such as pesticide residues, drug resistance, environmental pollution, etc., which have a serious threat to the safety of rape production [5–7]. Carbendazim and acetamidine are widely used to control pests and diseases in oilseed rape. They can improve the yield and quality of oilseed rape and ensure the economic benefits of farmers. However, if used incorrectly or in excess, it may remain in crops and have an impact on human health and the environment. Therefore, it is urgent to develop rapid, accurate and sensitive detection methods of carbendazim, acetamidine and other pesticides.

At present, the commonly used pesticide residue detection methods include chromatography, enzyme inhibition and biosensor detection [8–10]. The chromatographic method has small sample amount, fast analysis speed and high detection sensitivity, but it is limited by molecular size, boiling point and other factors, so the separation effect of polar substances is poor, and limited in detection

---

[11]. The specificity of enzyme inhibition method needs to be further improved, and the sample substrate also has certain influence on enzyme activity [12]. Biosensors have the advantages of high selectivity, portability and automation, but the production process is complicated and the cost is high. In recent years, the rapid development of instrument technology makes the spectral analysis and detection technology in agriculture, food detection widely used [13–15]. Compared with the traditional chromatography, enzyme inhibition method, biosensor method, surface enhanced Raman spectroscopy has the advantages of fast detection speed, high sensitivity, low detection limit.

Raman technology includes Raman spectroscopy and various derivative methods. It is a kind of scattering spectrum characterized by molecular vibration and rotation [16]. When the excited light and analyte molecules collide inelastic, the scattered light of different wavelengths is generated, and the scattered light of higher wavelength is collected to form Raman spectrum. Each molecular structure has its unique fingerprint characteristics of Raman spectrum, which makes Raman spectrum has important application value in the analysis of molecular structure [17]. The phenomenon was first discovered by Raman in 1928. SERS was originally discovered in 1974 by Fleischmann et al. who observed that the Raman signal of pyridine molecules adsorbated on rough silver surfaces was much stronger than that of pyridine molecules adsorbated in solution. Surface-enhanced Raman spectroscopy (SERS) techniques significantly enhance the Raman signal compared to conventional Raman spectroscopy, thereby improving the sensitivity of SERS substrates.

Currently, researchers attribute surface-enhanced Raman scattering to two mechanisms: electromagnetic enhancement and chemical enhancement. In electromagnetic enhancement, local electromagnetic field enhancement caused by surface plasmon resonance is considered to be the most important contribution. Surface plasmon is the collective oscillation effect of free electrons in metal under the photoelectric field. Selecting appropriate excitation wavelength can greatly improve the intensity of electromagnetic field [18,19]. The chemical enhancement is attributed to the fact that when molecules are chemically adsorbed on the substrate surface, surface adsorbed atoms and other co-adsorbed species may have certain chemical interactions with molecules. These factors have a direct impact on the electron density distribution of molecules, that is, the change of system polarizability affects its Raman strength [20,21].

Microfluidic technology is a technique to study the behavior and control of micro fluid. It controls the flow and mixing of liquids at the micron scale by placing fluids in micron scale channels. Compared with traditional laboratory technology, microfluidic technology has the advantages of high throughput, high sensitivity, small size, low cost, automation and integration [22–24]. In recent years, Raman spectroscopy and surface-enhanced Raman spectroscopy are combined with microfluidic chip, showing their unique complementary advantages. The laser spot can penetrate the transparent chip, so as to realize the non-destructive, in situ, online, and multi-target detection on the chip, with high resolution, fast speed, high sensitivity, good repeatability, and high degree of automation [25,26]. Gauthier Emonds-Alt et al. combined SERS with a microfluidic system to develop, optimize and validate methods for the determination of glyphosate in tap water. The microfluidic setup was optimized, the microfluidic design was constructed for the configuration of this application to integrate the SERS substrate synthesis into the detection of analytes, and the experimental design method was used to maximize the SERS signal of glyphosate. The limits of glyphosate were 40 μg/L and 78 μg/L, respectively. The recoveries ranged from 76 % to 117 %, and the reproducibility and disunity were less than 17 %. AMPA and glyphosate were simultaneously detected in tap water [27]. Xuan He et al. developed an ultra-sensitive and reusable SERS microfluidic biosensor with UO^{2+} response characteristics, prepared an aptamer-modified zinc-silver hybrid array by colloidal crystal template method, and applied it to high-performance sensor UO^{2+} with detection limit as low as 7.2×10^{-13} M. It is nearly five orders of magnitude lower than the maximum pollution level set by the Environmental Protection Agency [28]. Microfluidic technology expands the application areas of Raman and surface-enhanced Raman spectroscopy to meet extensive testing requirements, opening up new opportunities for integration and miniaturization of analysis platforms [29].

In this paper, a fast, accurate and reliable method was proposed. The SERS microfluidic chip technology was used to prepare the SERS substrate of Ag-Ps microspheres by spin coating and magnetron sputtering deposition of Ag. The PDMS microfluidic chip was designed and the SERS substate was bonded for detection. The linear parameters R^2 of carbendazim and acetamidine were 0.987 and 0.994, respectively, and the minimum detection limit was 0.01 mg/mL. The detection principle is shown in Fig. 1.
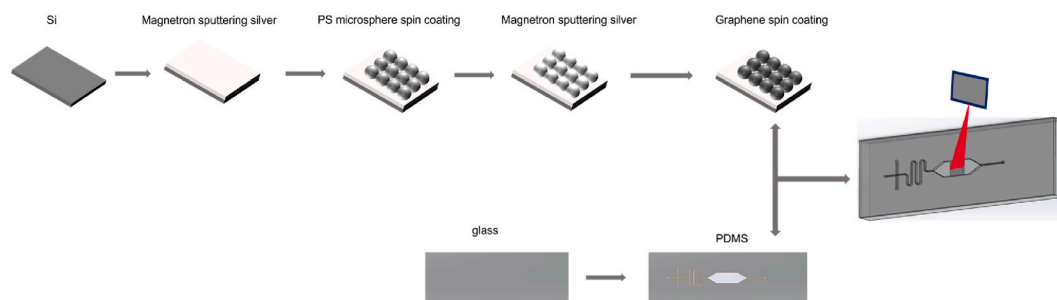

Fig. 1. Fabrication and detection of SERS microfluidic chip.

2. Experimental section

2.1. Materials

Domestic monodisperse polystyrene microsphere solution; N-type silicon substrate with crystal phase <110>; 99.99 % pure silver target; R6G; Graphene oxide (GO); Polydimethylsiloxane (PDMS); SU-8 3035 photoresist; Polyethylene glycol (PEG); PTFE catheter; Carbendazim powder standard sample, acetamidine powder standard sample; Methanol, acetone, anhydrous ethanol, dilute hydrochloric acid from the laboratory, are analytically pure; Deionized water was used in all experiments.

2.2. Preparation of SERS base for PS microsphere arrays

First, a four-inch silicon wafer is cut into a cube shape of 1.5 cm by 1.5 cm using a silicon wafer knife. Then, the cut silicon wafers were cleaned with acetone, anhydrous ethanol, dilute hydrochloric acid and deionized water for 5min in turn. Finally, a large amount of deionized water was used for washing, and the surface of the silicon wafers was dried with nitrogen. Magnetron sputtering 100 nm thick silver film on the treated silicon substrate as the reflective layer. During the self-assembly of PS microspheres with a diameter of 200 nm, the concentration of dispersing liquid and the spin coating speed have a great influence on the array structure. Therefore, different concentrations and different rotation speeds are selected for the experiment to achieve the optimal effect. Before spinning coating, the substrate is placed in a plasma cleaning machine, and plasma treatment is carried out for 1min to improve the hydrophilicity of the silicon wafer. Then the silicon substrate with improved hydrophilicity was placed on the suction cup of the glue levelling machine, the vacuum pump was opened, the silicon wafer was fixed on the suction cup, and the rotational speed of the glue levelling machine was adjusted. The rotational coating time was 15s–20s. After the above experiments were prepared, 20 - 40 μl of PS microsphere dispersing liquid of different concentrations was dropped on the silicon wafer with a pipette gun. After dispersing liquid spread all over the silicon wafer, spin coating was started. The optimal spin coating effect was achieved by adjusting different spin coating speed. The single layer PS microsphere array structure prepared above is used as template, and placed into the magnetron sputtering coating machine. The current is adjusted to about 50A, and the magnetron sputtering 60 nm thick precious metal silver is used as the active layer, thus greatly improving the Raman signal intensity. On the basis of the prepared Ag-PS microspheres SERS base, 10 mg of GO was dissolved in 100 mL deionized water, and then ultrasonic mixing was carried out to make GO completely dissolved in water, and 0.1 mg/mL of GO aqueous solution was obtained. Then a pipette was used to absorb 20 μl of GO aqueous solution and add it to the surface of SERS base. The rotational speed of the homogenizer was set as 1200r/min for 10s and 2500r/min for 30s, so that the GO aqueous solution was evenly distributed on the surface of SERS base. Finally, the SERS substrate coated with GO was heated at 80 °C for 20min to obtain Go-Ag-Ps microspheres SERS substrate.

2.3. Microfluidic chip preparation

According to the microfluidic microchannel structure, the drawing is designed in AutoCAD, and the mask plate is made by UV lithography technology. Before PDMS inverted mold, mold surface needs to be treated, mold surface should be clean, smooth, free of dust and impurity. The mold surface should also be modified with silanization, to avoid the adhesion of PDMS on the mold. A syringe was used to drain 40 g of PDMS into a plastic beaker. Then take PDMS curing agent 4 g in plastic beaker according to the ratio of PDMS to curing agent 10:1. A glass stirring rod was used to stir for 30min, and thoroughly mix PDMS and curing agent. After the stirring is completed, many tiny bubbles will be produced in the mixture. Place the plastic beaker containing the PDMS mixture in a vacuum oven. Open the exhaust valve to draw out the air in the oven. When the vacuum inside the box reaches the vacuum standard, close the exhaust valve. During the vacuum period, the PDMS mixture will expand, and pay attention to prevent the mixture from overflowing. After vacuum for 30min, the air bubbles in the mixture have disappeared. The treated PDMS mixture is coated on the silicon mold and placed in a vacuum oven. At 80 °C, it was cured for 1 h. After curing, the cured PDMS cover sheet is peeled off from the silicon template. After salinizing the silicon template, the PDMS can be directly peeled off from the silicon template. Then the cured PDMS were cut to obtain the PDMS cover. Then, a hole punch was used to punch holes in the corresponding positions on the PDMS cover sheet. The finished PDMS cover sheet and glass substrate were soaked in ethanol and isopropyl alcohol solution successively, cleaned by ultrasonic cleaning instrument for 10min, and then taken out on an electric heating plate and dried at 50 °C. Avoid dust during cleaning and drying. Put the dried PDMS cover sheet and glass substrate into the plasma cleaning machine, plasma treatment 45s, improve the hydrophilicity of the surface of both, take out the PDMS cover sheet and glass substrate bond, microfluidic chip production is completed.

2.4. SERS microfluidic chip bonding

The glass base of microfluidic was 7.5cm × 2.5cm × 0.2 cm. A square area with an area of 0.5cm × 0.5 cm and a depth of 0.5 mm was cut out by CNC technology in the corresponding detection area, which was used for placing SERS base. The SERS base of the GO-Ag-PS microspheres prepared was placed in the testing area, the glass base and the PDMS cover were cleaned in the plasma cleaning machine for 45s, the surface hydrophilicity of the glass base and the PDMS cover was significantly improved, and the SERS base was taken out of the plasma cleaning machine, placed in the testing area and pasted together immediately. After completion of bonding, punch holes at the inlet and outlet and insert PTFE catheter. The prepared SERS microfluidic chip physical object had a fishbone structure, and its center part was the SERS detection area. The liquid inlet and outlet were connected by PTFE hose, and the liquid to be

measured was injected into the microfluidic channel through PTFE hose, and tested in the test area.

2.5. SERS substrate characterization

Under 3 kV accelerated voltage, the morphology of SERS base was characterized by scanning electron microscopy (SEM). The SERS spectrum was obtained using a micro confocal Raman spectrometer equipped with a 785 nm laser beam. The laser power was set to 30 mW, the integration time was set to 5s, and the objective magnification was adjusted to 10 times.

2.6. SERS microfluidic chips test

Configure R6G water solution with a concentration of 10^{-2} M, and successively dilute the concentration gradient by 10 times to 10^{-14} M. R6G solution with a concentration of 10^{-6} M was injected into the SERS microfluidic chip. After the R6G solution flowed to the detection area, the microfluidic chip was placed on the electric heating table to dry for SERS test. The function of SERS intensity of R6G characteristic peak at 1506 cm^{-1} as a function of concentration on logarithmic scale was drawn, and their linear relationship was further fitted into a working curve. In addition, the uniformity and reproducibility of the prepared SERS microfluidic chips were evaluated.

2.7. The SERS detection of carbendazim and acetamidine

Preparation of carbendazim standard solution: Weigh 0.01 g carbendazim standard powder and dissolve it into 10 mL methanol to prepare 1000 mg/L carbendazim standard solution, and then dilute it successively into 100, 10, 1, 0.1, 0.01 mg/L gradient standard solution.

Preparation of acetamidine standard solution: Weigh 0.01 g acetamidine standard powder and dissolve it in 10 mL methanol to prepare 1000 mg/L acetamidine standard solution, and then dilute it successively to 100, 10, 1, 0.1, 0.01 mg/L gradient standard solution.

Carbazim standard solution and acetamidine standard solution were injected into the injection port of SERS microfluidic chip through a syringe respectively, and sat for a few minutes. The standard solution flowed to the SERS detection area, and Raman spectrum of the standard solution was collected by Raman spectrometer at room temperature. Incident laser wavelength is 785 nm, laser power is 30 mW, 50 times objective lens is selected, spectrum acquisition time is 5S, integration times is 2, 10 spectra of each kind of sample are collected each time, OMINC software is used to obtain the average value of 10 spectra collected as the original spectrum of this concentration. After the collection is completed, OMINC software is used for processing.

2.8. SERS substrate simulation

According to SERS substrate design and production material, relevant parameters of simulation were set: the base plate of SERS substrate was monocrystalline silicon slice, and the thickness was set as 0.5 μm; A layer of metal made of Ag is arranged on the silicon wafer as the reflecting layer, the thickness of which is 0.1 μm. The size of the silver nanospheres is set at 260 nm in the center of the substrate, and the gap is 2–12 nm. The excitation wavelength is 785 nm and the incident mode is z-backward. The mesh size is set to 4 nm. The boundary conditions in the X and Y directions are periodic boundary conditions, and the boundary conditions in the Z axis direction are perfect matching layer. The surrounding medium of SERS base was air, and the background refractive index was 1.

3. Results and discussion

3.1. Characterization of SERS substrate

The prepared SERS substrate was characterized by SEM, and the result was shown in Fig. 2. From the SEM image, Ag film was
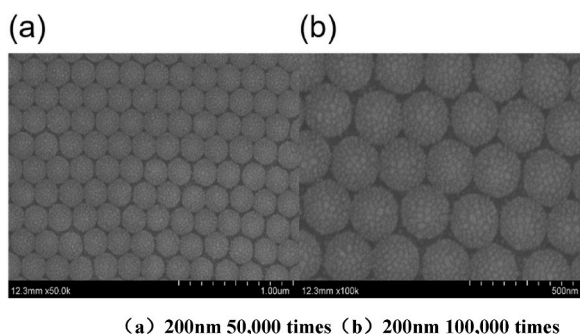

（a）200nm 50,000 times （b）200nm 100,000 times

Fig. 2. SEM images of PS microspheres after Ag deposition.

sputtered to the top of PS microsphere, and the silver nanostructure presented a cluster-like shape instead of a flat geometric structure. Compared with the flat precious metal film, the cluster-like silver nanostructure greatly improved the surface roughness and contact area of SERS substrate, which could attach more molecules of the object to be tested and produce a stronger enhancement effect. Ag nanoparticles are uniformly distributed on the surface of PS microspheres, and the number and intensity of hot spots are greatly improved by the tiny gaps between the nanoparticles, which greatly enhances the Raman signal.

3.2. SERS substrate simulation

The PS microsphere-Ag structure was studied using the FDTD method to simulate the distribution of electromagnetic fields in PS microsphere-Ag nanoparticle arrays. The influence of the distance variation between silver nanoparticles on the enhancement of the electromagnetic field was investigated. It has been demonstrated that the deposition of 60 nm Ag nanoparticles significantly enhances the electric field. Therefore, the effect of the spacing between 2 and 12 nm (different nanospacing) on the enhancement of the electric field was analyzed. A model was established using 60 nm Ag nanoparticles as the simulation object, with the simulation parameters being the same as those mentioned above.

As shown in Fig. 3, it is the electromagnetic field intensity color distribution map at different spacing of 200 nm PS microspheres array, and the incident light is at 785 nm. The electric field with a spacing of 2 nm is about 41 V/m at its strongest, and that with a spacing of 12 nm is about 19 V/m. The electromagnetic fields with a spacing of 2–12 nm are 41 V/m, 34 V/m, 31 V/m, 31 V/m, 28 V/m, and 19 V/m in turn. Plot the relation between different spacing and the intensity of electromagnetic field, and the results are shown in Fig. 4. The results show that the electric field enhancement effect is stronger with the decrease of Ag particle spacing.

3.3. Sensitivity of SERS substrate

R6G probe molecules were used for SERS performance detection. R6G aqueous solution with a concentration of 10^{-2} M was configured, and the concentration gradient was diluted 10 times successively to 10^{-14} M. The above R6G solution with different
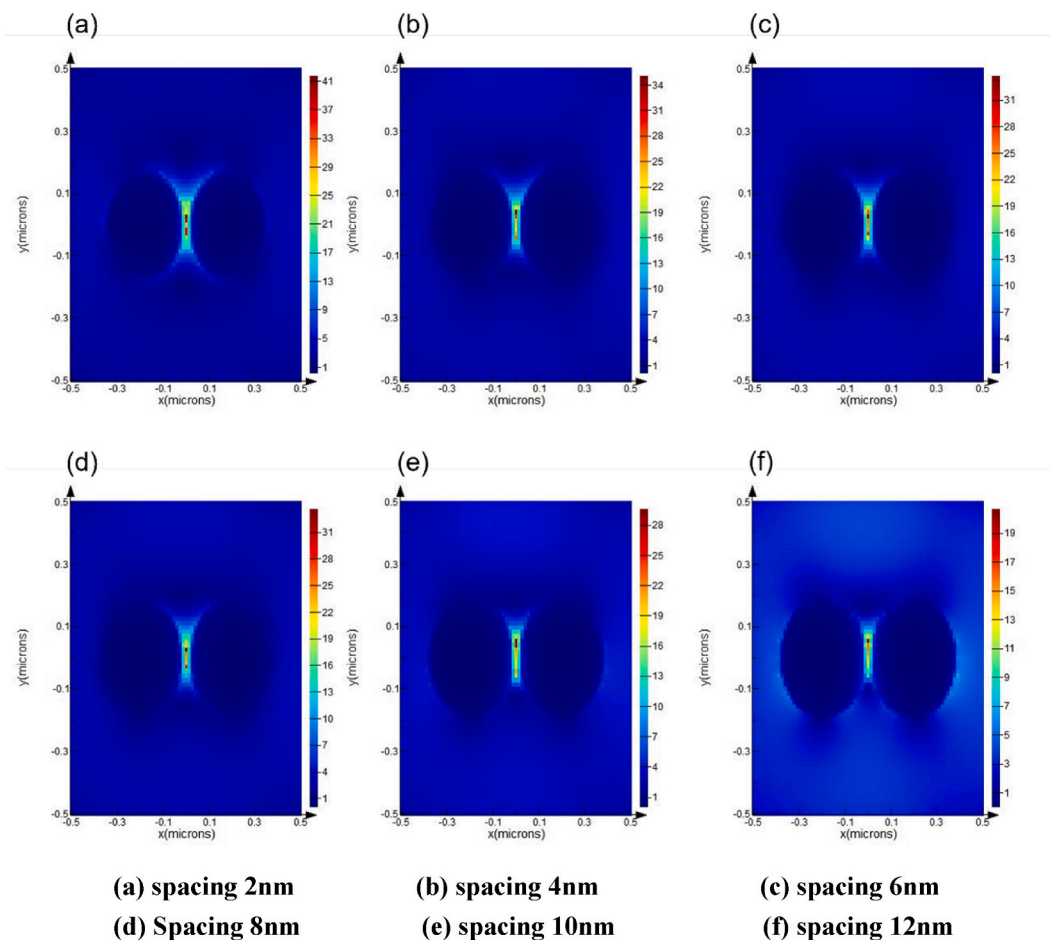

(a) spacing 2nm (b) spacing 4nm (c) spacing 6nm
(d) Spacing 8nm (e) spacing 10nm (f) spacing 12nm

Fig. 3. Electric field intensity of 200 nm PS microspheres with a spacing of 2–12 nm.
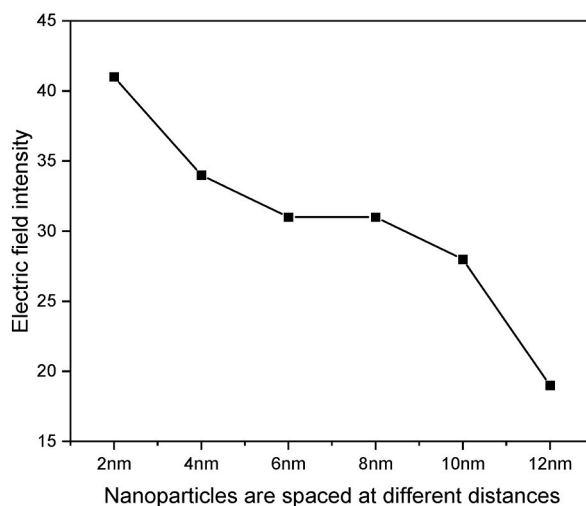
Fig. 4. Relationship between electric field intensity and nanoparticle spacing.

concentrations was added to SERS substrate by drops respectively, and the substrate was placed on the heating table with the temperature set at 80 °C. Raman spectrum was collected after the solvent was dried, as shown in Fig. 5.

The Raman spectrum has a characteristic peak at 610 cm^{-1},770 cm^{-1}, 1181 cm^{-1},1307 cm^{-1}, 1359 cm^{-1},1506 cm^{-1},1644 cm^{-1}, which is consistent with the Raman characteristic peak of R6G, and represent C–H plane bending, carbon ring vibration and C–C bond stretching in R6G molecule, respectively. As the concentration of R6G aqueous solution continues to decrease, its corresponding Raman spectrum intensity gradually decrease. Fig. 5(a) shows the Raman spectrum of R6G at 10^{-2}-10^{-12} M. When the concentration of R6G aqueous solution was as low as 10^{-12} M, the corresponding Raman characteristic peak could still be detected under the low laser power of 30mw, that is, the R6G detection limit is 10^{-12} M.

Fig. 5(b) took the concentration of R6G solution as the abscissa and the SERS characteristic peak intensity value at 1506 cm^{-1} of the Raman spectrum of R6G as the ordinate to calculate the standard curve. The linear equation established is y = 3325.8x+43810.7, where x is the logarithm of R6G concentration, the linear correlation is R^2 = 0.986, the linear range is 10^{-2}-10^{-12} M, and the detection limit is 10^{-12} M.

Table 1 shows the stretching vibration of chemical bonds corresponding to different Raman shifts of R6G, which is basically consistent with the published data.

In SERS technology, enhancement factor (EF) is one of the key parameters to measure the effect of signal enhancement. The enhancement factor can be used to compare the SERS performance of different base materials, and also to evaluate the SERS signal enhancement effect under different experimental conditions. The calculation formula is as follows:
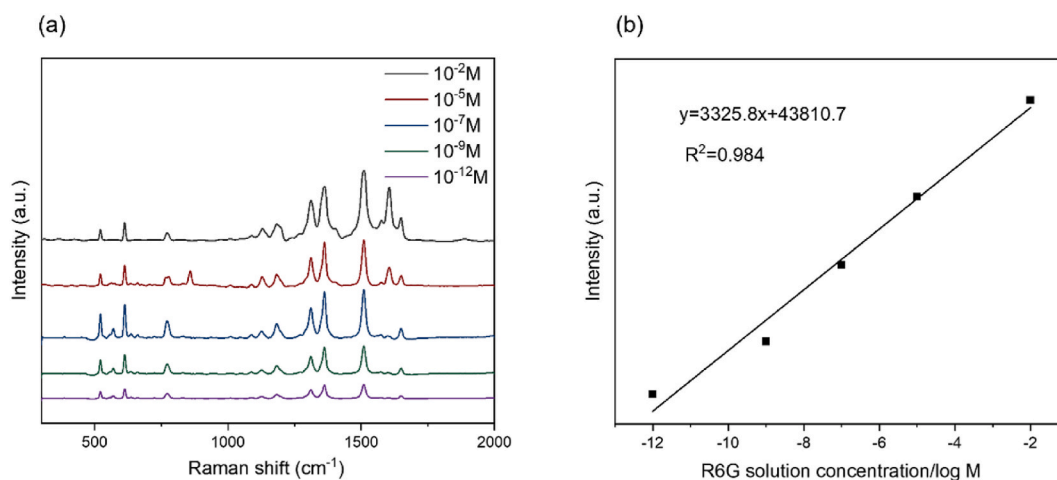

Fig. 5. (a) SERS substrate detection spectrum of R6G with different concentrations(b) Relationship between the intensity of the Raman characteristic peak of R6G at 1506 cm^{-1} and the logarithmic concentration of R6G.

Table 1
Raman SERS spectra and peak distribution of R6G.

Characteristic peak	Raman shift/cm^{-1}	Peak attribution
1	610	C–C–C intratorus deformation
2	770	C–H bending vibration
3	1181	C–C stretching vibration
4	1307	C–H stretching vibration
5	1359	N–C–C stretching vibration
6	1506	C–C stretching vibration
7	1644	C–O stretching vibration

$$EF = \frac{I_{SERS} \times N_{bulk}}{I_{bulk} \times N_{SERS}}$$

I_{SERS} refers to the Raman spectral intensity of R6G on the SERS base, I_{bulk} refers to the Raman spectral intensity of R6G on the common base without enhancement, N_{bulk} refers to the amount of R6G molecules adsorbed on the common base, and N_{SERS} refers to the amount of R6G molecules adsorbed on the SERS base of Ag-PS microspheres. In this paper, R6G solution of 10^{-6} M was selected for testing and analysis, and enhancement factor was calculated at 1506 cm^{-1}. I_{SERS} and I_{bulk} could be obtained directly from Raman spectrum, so it was mainly necessary to calculate the value of N_{bulk} and N_{SERS}. The N_{bulk} calculation formula is as follows:

$$N_{bulk} = cAh$$

The laser wavelength is 785 nm and the laser power is about 30 mW. In the formula, c is the concentration of R6G is 10^{-6} M, and A is the area of the laser spot, which is about 10 μm^2. h is the penetration depth of laser and is related to laser wavelength. In this experiment, h should be 15 μm. The calculation formula of N_{SERS} is as follows:

$$N_{SERS} = \frac{C_{lim}VA}{\pi r^2}$$

where, C_{lim} is the lowest concentration of R6G solution, V is the volume of R6G solution added on the SERS base by drops (30 μL in the experiment), A is the area of laser spot, πr^2 is the area of circular region formed by R6G solution on the SERS base. Finally, the enhancement factor of Ag-PS microsphere SERS base on R6G at 1506 cm^{-1} was up to 2.4×10^{10}.

3.4. Detection limits of SERS microfluidic chip

R6G solution with a concentration of 10^{-2} M was prepared, diluted 10 times to 10^{-14} M successively, and R6G solution of the same volume (10^{-2}-10^{-14} M) was injected into SERS microfluidic chip successively. The laser power was set as 30 mW, and the integration time was 5s for detection. Five Raman spectra of R6G solution with different concentrations were collected and averaged as SERS spectra of this concentration. As shown in Fig. 6, Raman characteristic peaks of 1307 cm^{-1}, 1359 cm^{-1} and 1506 cm^{-1} of R6G solutions with different concentrations can be clearly seen. As the concentration of R6G solution decreases, the corresponding Raman spectral intensity decreases gradually. When the concentration of R6G aqueous solution was as low as 10^{-11} M, the corresponding Raman characteristic peak could still be detected under the low laser power of 30mw, that is, the R6G detection limit of the SERS microfluidic
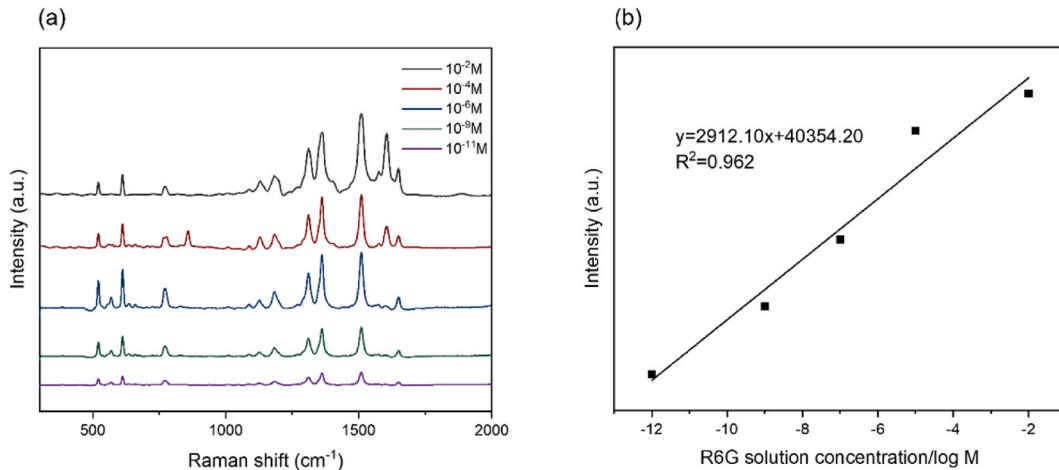
Fig. 6. (a)SERS microfluidic chip detection spectrum of R6G with different concentrations (b) Relationship between the intensity of the Raman characteristic peak of R6G at 1506 cm^{-1} and the logarithmic concentration of R6G.

chip was as low as 10^{-11} M.

Fig. 6(b) took the concentration of R6G solution as the abscissa and the SERS characteristic peak intensity value at 1506 cm^{-1} of the Raman spectrum of R6G as the ordinate, and calculated the standard curve of SERS microfluidic chip detecting R6G. The linear equation established is y = 2912.10x+40354.20, where x is the logarithm of R6G concentration, the linear correlation is R^2 = 0.962, the linear range is 10^{-2}-10^{-11} M, and the detection limit is 10^{-11} M. The results showed that there was a good linear relationship between peak intensity and concentration within the range of low concentration, which could be used for quantitative detection of pesticide residues. Moreover, the SERS microfluidic chip was highly sensitive and could be used for detection of pesticide residues.

In the process of detecting R6G using a SERS microfluidic chip, the R6G solution is injected into the microfluidic channel through the inlet, and allowed to flow spontaneously along the channel walls by capillary force after waiting for the solution to pass through the capillary channel. Then, it flows into the detection area, which is the SERS substrate, and Raman spectroscopy is used to collect Raman signals from the SERS microfluidic chip. Upon completion of the collection, the solution also flows out of the microfluidic channel through the outlet. Organic solvents such as ether or ethanol are then injected into the microfluidic channel to wash away any remaining R6G solution. Deionized water is washed in the same manner once more to ensure the reusability and sensitivity of the SERS microfluidic chip.

In the study, the R6G solution is dried on a desiccator before testing the uniformity and repeatability of the SERS microfluidic chip to prevent the solution from drying and solidifying during the Raman signal acquisition process, which could result in the incomplete collection of signals from the 10 points due to the solution flowing out of the channel before the acquisition is finished. Drying is not always necessary to prevent insufficient detection time or inadequate solution flow.

When detecting different concentrations of pesticide residues, the solutions are usually from different batches of SERS microfluidic chips because the SERS microfluidic chips produced are low-cost and can be mass-produced in large batches. However, for testing repeatability, the same SERS microfluidic chip needs to be used.

3.5. Microfluidic chip structure

A pump-free PDMS microfluidic chip was designed. The chip size is 45mm × 20mm × 5 mm, as shown in Fig. 7. Microfluidic chip consists of three parts. Three liquid inlet ports are set to realize mixing and detection of various substances in the microchannel. The chaotic advection effect is generated because the fluid is constantly stretched and folded during the flow process, which can increase the mixing degree of the solution. Therefore, the mixing effect of liquid can be enhanced by the use of serpentine channels. The detection area was fishbone structure with better liquid fluidity and collection performance, and its area was larger than other areas, so SERS base was embedded in this area for convenience of detection. At the outlet, the tested solution is discharged from the outlet, and the microfluidic channel is repeatedly cleaned with deionized water to make it reusable.

In general, different liquids under test are added to multiple intakes respectively at the same time. Under the action of liquid surface tension and capillary force, the liquids under test will quickly flow into the snake channel. In the serpentine channel, the three liquids under test are thoroughly mixed by centrifugal force. Then it flows into the detection area for detection, and then flows out of the outlet after detection. The microchannel is repeatedly cleaned with deionized water for reuse.

3.6. Uniformity and reproducibility of SERS microfluidic chip

The microfluidic chip was used for mixing samples, where a certain volume of solution was withdrawn and injected into the inlet of the SERS microfluidic chip via a syringe. After allowing the mixture to stand for a few minutes, the combined solution was drawn to the SERS detection area under the capillary action, enabling the mixing within the microfluidic channels and the detection of various substances. The use of serpentine channels enhanced the mixing of the liquid, as the fluid was continuously stretched and folded during its flow, thereby increasing the degree of solution mixing. Raman spectroscopy was performed on the standard solution at room temperature using a Raman spectrometer. In practical application, it is crucial to prepare SERS microfluidic chips with good uniformity and reproducibility. Therefore, this section tested the uniformity, reproducibility and other aspects of the SERS microfluidic chips prepared above. R6G solution with a concentration of 10^{-6} M was injected into the SERS microfluidic chip. After the R6G solution flowed spontaneously to the detection area. Ten detection points were selected within the detection area for spectral collection, and the experimental results were shown in Fig. 8. There was almost no difference in SERS spectrum of R6G molecules, indicating that the
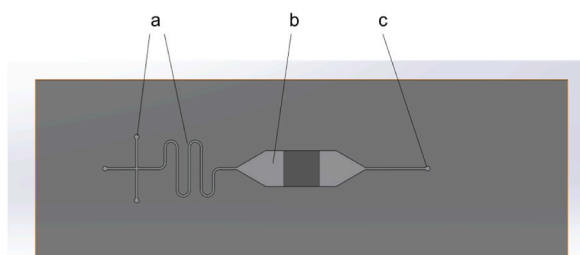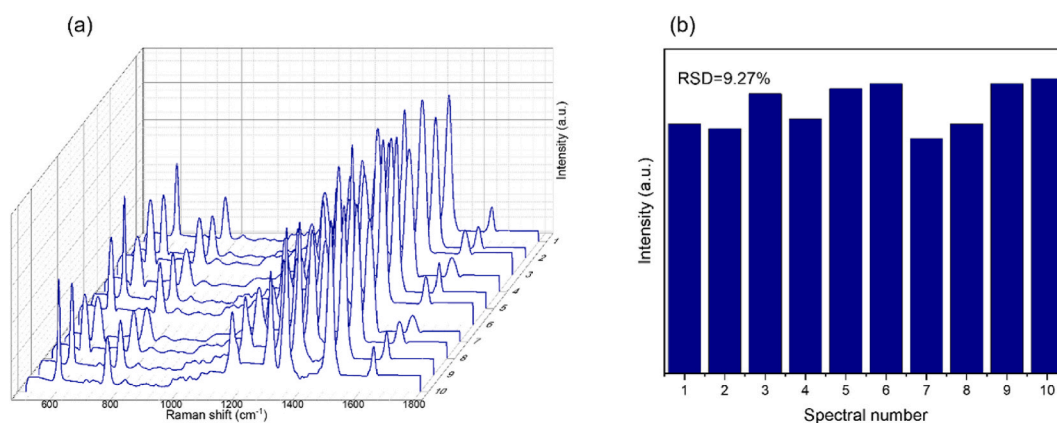

Fig. 7. Microfluidic structure diagram.

Fig. 8. (a)SERS spectra of R6G solution with 10^{-6} M concentration tested at 10 detection points in microfluidic chip(*b*)Intensity distribution of characteristic peak of R6G at 1506 cm^{-1}.

SERS microfluidic chip had good uniformity. The intensity of Raman characteristic peaks at 1506 cm^{-1} of the Raman spectra of 10 detection points was compared, and the results were shown in the figure, with the relative standard deviation RSDS of 9.27 %.

In order to verify the reproducibility of the chip, 10 SERS microfluidic chips were prepared in this paper, and R6G solution with a concentration of 10^{-6} M was injected into each chip. The test method was the same as above, R6G signal was detected in SERS detection area of each chip. The results showed that there was little difference in SERS spectrum of R6G among the 10 SERS microfluidic chips, indicating that the SERS microfluidic chip designed had good reproducibility. According to the data in Fig. 9, the Raman peak intensity at 1506 cm^{-1} detected by 10 SERS microfluidics chips was statistically compared, and the relative standard deviation was 8.95 %.

3.7. Detection of carbendazim and acetamidine pesticides

The sensitivity of SERS microfluidic chip was investigated. Fig. 10 shows that the Raman signal strength at the corresponding characteristic shift decreases as the concentration of acetamidine reduces. When the concentration of carbendazim solution was as low as 0.01 mg/L, the characteristic peak of carbendazim molecule was still clearly visible at 1365 cm^{-1}. Therefore, the detection limit of SERS microfluidic chip for carbendazim standard sample could reach 0.01 mg/L. Taking the concentration of carbendazim solution as the abscissa and the intensity value of Raman characteristic peak at 1365 cm^{-1} of SERS spectrum as the ordinate, the standard curve of carbendazim detection on SERS microfluidics chip was calculated. The results are shown in Fig. 10(b). The Raman intensity at 1365 cm^{-1} had a good linear relationship with carbendazim concentration, and the correlation coefficient could reach 0.987.

Fig. 11 shows the Raman spectra of different concentrations of the standard solution of acetamidine. The Raman intensity of Mycorim at the characteristic shift decreases with the decrease of the detection concentration. When the concentration of acetamidine solution is as low as 0.01 mg/L, the characteristic peak of acetamidine molecule is still clearly visible at 1108 cm^{-1}. The results indicated that the detection limit of SERS microfluidic chips for acetaminidine standard samples could reach 0.01 mg/L. Taking the concentration of acetamidine solution as the abscissa and the intensity value of Raman characteristic peak at 1108 cm^{-1} of the SERS spectrum as the ordinate, the standard curve of detection of acetamidine on SERS microfluidic chip was calculated, and the result was shown in Fig. 11(b). Among them, the signal intensity at 1108 cm^{-1} and has a good linear relationship with the concentration of acetamidine, the correlation coefficient can reach 0.994.

4. Conclusions

In summary, we proposed a fast, accurate and reliable method for detecting carbendazim and acetamidine using SERS microfluidic chip technology. Ag-PS microsphere SERS substrate was prepared by spin coating and magnetron sputtering deposition. PDMS microfluidic chip was designed and SERS substrate was combined for the detection of carbendazim and acetamidine Compared with traditional colorimetric method, gas chromatography, liquid chromatography and other methods, the SERS method proposed in this paper has obvious advantages such as simple sample pretreatment, fast reaction speed and reliable result. The working curves were well fitted, the linear parameters R^2 were 0.987 and 0.994, respectively, and the minimum detection limit was 0.01 mg/mL. Therefore, the use of SERS microfluidic chips to detect carbendazim and acetamidine is expected to provide a way for the detection of pesticide residues in crops, which has broad application prospects in the field of food safety.

## CRediT authorship contribution statement

Wang Peng: Writing – review & editing, Writing – original draft, Methodology, Conceptualization. **Zhihan Xu:** Writing – original draft, Formal analysis, Data curation. **Chao Yi:** Validation, Data curation. **Yuankai Zhang:** Validation. **Qingxi Liao:** Supervision.
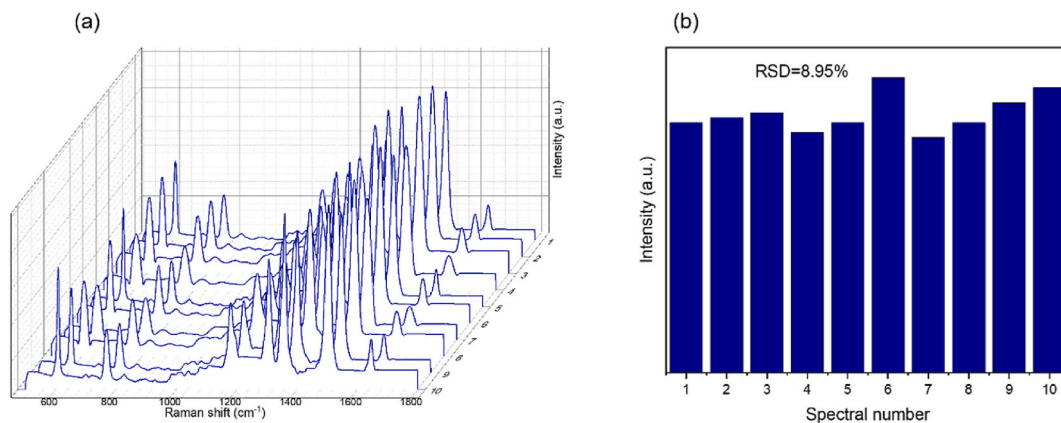
Fig. 9. (a)SERS spectra of R6G solution with 10^{-6} M concentration tested at 10 detection points in microfluidic chip(*b*)Intensity distribution of characteristic peak of R6G at 1506 cm^{-1}.
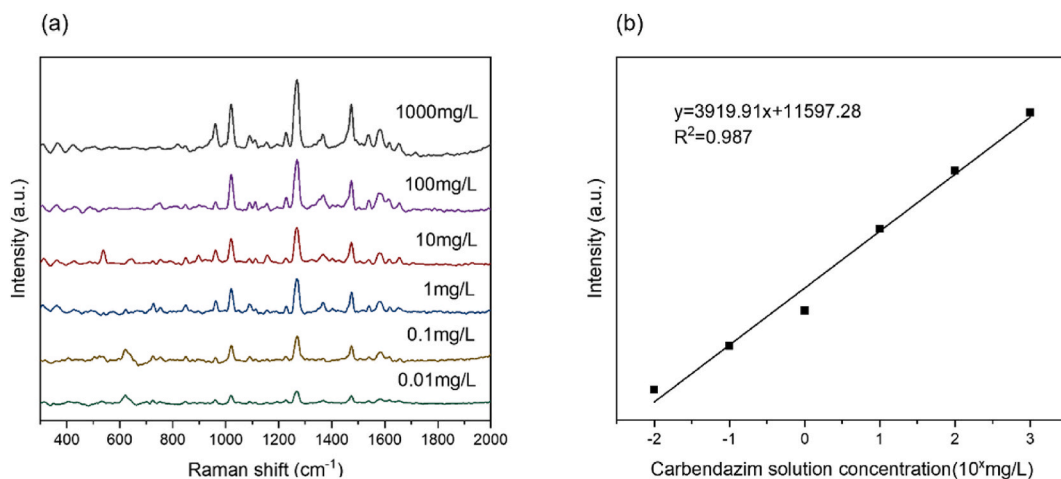
Fig. 10. (a) SERS spectra of carbendazim standard solution with different concentrations (b) The relationship between the strength of the Raman characteristic peak of carbendazim at 1365 cm^{-1} and the solution concentration.
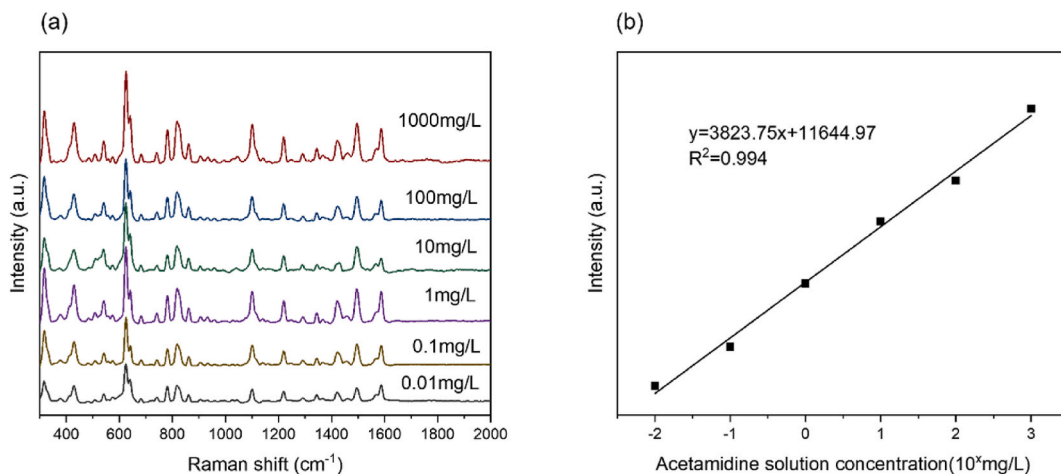
Fig. 11. (a) SERS spectrogram of acetamiprid standard solution with different concentrations (b) The relationship between the intensity of the Raman characteristic peak of acetamiprid at 1108 cm^{-1} and the concentration of the solution.

Declaration of competing interest

The authors declare that they have no known competing financial interests or personal relationships that could have appeared to influence the work reported in this paper.

Acknowledgements

References

[1] X. Wen, C. Ma, M. Sun, Y. Wang, X. Xue, J. Chen, W. Song, H. Li-Byarlay, S. Luo, Pesticide residues in the pollen and nectar of oilseed rape (Brassica napus L.) and their potential risks to honey bees, Sci. Total Environ. 786 (2021) 147443.

[2] R. Cech, J.G. Zaller, A. Lyssimachou, P. Clausing, K. Hertoge, C. Linhart, Pesticide drift mitigation measures appear to reduce contamination of non-agricultural areas, but hazards to humans and the environment remain, Sci. Total Environ. (2022) 158814.

[3] Z. Lian, X. Gu, L. Liu, X. Zhao, Diffuse phthalate acid esters losses induced from large amount of agricultural plastic film residues caused low risks for water quality in China during 1991-2017, J. Hazard Mater. 431 (2022) 128644.

[4] S.X. Liang, H. Li, Q. Chang, R. Bai, Z. Zhao, G.F. Pang, Residual levels and dietary exposure risk assessment of banned pesticides in fruits and vegetables from Chinese market based on long-term nontargeted screening by HPLC-Q-TOF/MS, Ecotoxicol. Environ. Saf. 248 (2022) 114280.

[5] T.O. Ajiboye, P.O. Oladoye, C.A. Olanrewaju, G.O. Akinsola, Organophosphorus pesticides: Impacts, detection and removal strategies, Environ. Nanotechnol. Monit. Manag. 17 (2022).

[6] Q. Fu, X. Jia, S. Zhang, J. Zhang, D. Sun-Waterhouse, C. Wang, G.I.N. Waterhouse, P. Wu, Highly defective copper-based metal-organic frameworks for the efficient adsorption and detection of organophosphorus pesticides: an experimental and computational investigation, Food Chem. 423 (2023).

[7] W. Jing, S. Qiang, Z. Jia, Q.H. Shi, X. Meng, M. Yu, H. Ma, K. Zhao, Y. Dai, Smartphone-integrated nanozymes sensor array for high throughput recognition of organophosphorus pesticides, Sensor. Actuator. B Chem. 389 (2023).

[8] V. Mingo, C. Leeb, A.K. Fahl, S. Lotters, C. Bruhl, N. Wagner, Validating buccal swabbing as a minimal-invasive method to detect pesticide exposure in squamate reptiles, Chemosphere 229 (2019) 529–537.

[9] T.W. Na, H.J. Seo, S.N. Jang, H. Kim, H. Yun, H. Kim, J. Ahn, H. Cho, S.H. Hong, H.J. Kim, S.H. Lee, Multi-residue analytical method for detecting pesticides, veterinary drugs, and mycotoxins in feed using liquid- and gas chromatography coupled with mass spectrometry, J. Chromatogr. A 1676 (2022) 463257.

[10] C. Benbrook, Missing the mark – new methods needed to detect and address high-risk pesticide residues in the global food supply, Regul. Toxicol. Pharmacol. 138 (2023) 105328.

[11] H.İ. Ulusoy, M. Sattari Dabbagh, M. Locatelli, S. Ulusoy, A. Kabir, M.A. Farajzadeh, Azinphos-methyl and chlorfenvinphos pesticides determination using fabric phase sorptive extraction followed by high performance liquid chromatography-photodiode array detector, Microchem. J. 191 (2023).

[12] J. Chang, H. Li, T. Hou, F. Li, Paper-based fluorescent sensor for rapid naked-eye detection of acetylcholinesterase activity and organophosphorus pesticides with high sensitivity and selectivity, Biosens. Bioelectron. 86 (2016) 971–977.

[13] W. Peng, Z. Xu, X. Jia, Q. Liao, A copper foam-based surface-enhanced Raman scattering substrate for glucose detection, Discover Nano 18 (1) (2023) 7.

[14] B. Sharma, R.R. Frontiera, A.I. Henry, E. Ringe, R.P. Van Duyne, SERS: materials, applications, and the future, Mater. Today 15 (1–2) (2012) 16–25.

[15] W. Peng, B. Huang, X. Huang, H. Song, Q. Liao, A flexible and stretchable photonic crystal sensor for biosensing and tactile sensing, Heliyon 8 (11) (2022) e11697.

[16] Shah, K. C., M. B. Shah, S. J. Solanki, V. D. Makwana, D. K. Sureja, A. K. Gajjar, K. B. Bodiwala and T.

[17] E.V. Solovyeva, O.V. Odintsova, V.O. Svinko, D.V. Makeeva, D.V. Danilov, Hydroxyapatite-nanosilver composites with plasmonic properties for application in surface-enhanced Raman spectroscopy, Mater. Today Commun. 35 (2023).

[18] Y. Zou, L. Jiang, T. Zhai, T. You, X. Jing, R. Liu, F. Li, W. Zhou, S. Jin, Surface-enhanced Raman scattering by hierarchical CuS microflowers: charge transfer and electromagnetic enhancement, J. Alloys Compd. 865 (2021).

[19] Z. Yang, L. Jiang, W. Zhao, B. Shi, X. Qu, Y. Zheng, P. Zhou, Nb2C MXene self-assembled Au nanoparticles simultaneously based on electromagnetic enhancement and charge transfer for surface enhanced Raman scattering, Spectrochim. Acta Mol. Biomol. Spectrosc. 299 (2023) 122843.

[20] Q. Wang, S. Lian, C. Guo, X. Gao, Y. Dou, C. Song, J. Lin, The chemical adsorption effect of surface enhanced Raman spectroscopy of nitrobenzene and aniline using the density functional theory, Spectrochim. Acta Mol. Biomol. Spectrosc. 279 (2022) 121428.

[21] N. Li, C. Wang, L. Li, Z. Hao, J. Gu, M. Wang, T. Jiao, Chemical gas sensor, surface enhanced Raman scattering and photoelectrics of composite Langmuir-Blodgett films consisting of polypeptide and dye molecules, Colloids Surf. A Physicochem. Eng. Asp. 663 (2023).

[22] K. Munirathinam, J. Park, Y.-J. Jeong, D.-W. Lee, Galinstan-based flexible microfluidic device for wireless human-sensor applications, Sensor Actuator Phys. 315 (2020).

[23] Z. Sheidaei, P. Akbarzadeh, N. Kashaninejad, Advances in numerical approaches for microfluidic cell analysis platforms, J. Sci.: Advanced Materials and Devices 5 (3) (2020) 295–307.

[24] Y. Zhao, X.G. Hu, S. Hu, Y. Peng, Applications of fiber-optic biochemical sensor in microfluidic chips: a review, Biosens. Bioelectron. 166 (2020) 112447.

[25] S. Halldorsson, E. Lucumi, R. Gomez-Sjoberg, R.M.T. Fleming, Advantages and challenges of microfluidic cell culture in polydimethylsiloxane devices, Biosens. Bioelectron. 63 (2015) 218–231.

[26] S. Hengoju, O. Shvydkiv, M. Tovar, M. Roth, M.A. Rosenbaum, Advantages of optical fibers for facile and enhanced detection in droplet microfluidics, Biosens. Bioelectron. 200 (2022) 113910.

[27] G. Emonds-Alt, C. Malherbe, A. Kasemiire, H.T. Avohou, P. Hubert, E. Ziemons, J.M. Monbaliu, G. Eppe, Development and validation of an integrated microfluidic device with an in-line Surface Enhanced Raman Spectroscopy (SERS) detection of glyphosate in drinking water, Talanta 249 (2022) 123640.

[28] X. He, X. Zhou, Y. Liu, X. Wang, Ultrasensitive, recyclable and portable microfluidic surface-enhanced Raman scattering (SERS) biosensor for uranyl ions detection, Sensor. Actuator. B Chem. 311 (2020).

[29] Y. Qasim Almajidi, S.M. Algahtani, O. Sajjad Alsawad, H. Setia Budi, S. Mansouri, I.R. Ali, M. Mazin Al-Hamdani, R. Mireya Romero-Parra, Recent applications of microfluidic immunosensors, Microchem. J. 190 (2023).